

## Article

# Immobilization of Recombinant Endoglucanase (CelA) from *Clostridium thermocellum* on Modified Regenerated Cellulose Membrane

Zi-Han Weng <sup>1,†</sup>, Parushi Nargotra <sup>2,†</sup>, Chia-Hung Kuo <sup>2,\*</sup>  and Yung-Chuan Liu <sup>1,\*</sup> <sup>1</sup> Department of Chemical Engineering, National Chung Hsing University, Taichung 402, Taiwan<sup>2</sup> Department of Seafood Science, National Kaohsiung University of Science and Technology, Kaohsiung 811, Taiwan

\* Correspondence: kuoch@nku.edu.tw (C.-H.K.); ycliu@dragon.nchu.edu.tw (Y.-C.L.); Tel.: +886-7-3617141 (ext. 23646) (C.-H.K.); +886-4-22853769 (Y.-C.L.)

† These authors contributed equally to this work.

**Abstract:** Cellulases are being widely employed in lignocellulosic biorefineries for the sustainable production of value-added bioproducts. However, the high production cost, sensitivity, and non-reusability of free cellulase enzymes impede their commercial applications. Enzyme immobilization seems to be a potential approach to address the aforesaid complications. The current study aims at the production of recombinant endoglucanase (CelA) originated from the cellulosome of *Clostridium thermocellum* in *Escherichia coli* (*E. coli*), followed by immobilization using modified regenerated cellulose (RC) membranes. The surface modification of RC membranes was performed in two different ways: one to generate the immobilized metal ion affinity membranes RC-EPI-IDA-Co<sup>2+</sup> (IMAMs) for coordination coupling and another to develop aldehyde functional group membranes RC-EPI-DA-GA (AMs) for covalent bonding. For the preparation of IMAMs, cobalt ions expressed the highest affinity effect compared to other metal ions. Both enzyme-immobilized membranes exhibited better thermal stability and maintained an improved relative activity at higher temperatures (50–90 °C). In the storage analysis, 80% relative activity was retained after 15 days at 4 °C. Furthermore, the IMAM- and AM-immobilized CelA retained 63% and 53% relative activity, respectively, after being reused five times. As to the purification effect during immobilization, IMAMs showed a better purification fold of 3.19 than AMs. The IMAMs also displayed better kinetic parameters, with a higher V<sub>max</sub> of 15.57 U mg<sup>-1</sup> and a lower K<sub>m</sub> of 36.14 mg mL<sup>-1</sup>, than those of AMs. The IMAMs were regenerated via treatment with stripping buffer and reloaded with enzymes and displayed almost 100% activity, the same as free enzymes, up to 5 cycles of regeneration.

**Keywords:** enzyme immobilization; recombinant endoglucanase; regenerated cellulose membrane; IMAM; immobilized metal ion affinity membrane



**Citation:** Weng, Z.-H.; Nargotra, P.; Kuo, C.-H.; Liu, Y.-C. Immobilization of Recombinant Endoglucanase (CelA) from *Clostridium thermocellum* on Modified Regenerated Cellulose Membrane. *Catalysts* **2022**, *12*, 1356. <https://doi.org/10.3390/catal12111356>

Academic Editor: Maria H. L. Ribeiro

Received: 8 October 2022

Accepted: 1 November 2022

Published: 3 November 2022

**Publisher's Note:** MDPI stays neutral with regard to jurisdictional claims in published maps and institutional affiliations.



**Copyright:** © 2022 by the authors. Licensee MDPI, Basel, Switzerland. This article is an open access article distributed under the terms and conditions of the Creative Commons Attribution (CC BY) license (<https://creativecommons.org/licenses/by/4.0/>).

## 1. Introduction

The ever-increasing reliance and over-exploitation of non-renewable fossil fuels, owing to accelerated urbanization and globalization, have led to their acute shortage, besides raising grave environmental concerns due to greenhouse gas emissions such as methane and carbon dioxide [1]. A large increase in methane emission (774 tera grams/year) due to tremendous anthropogenic activities has been reported. Additionally, the adverse effects of methane as a greenhouse gas are roughly 25 times greater than those of carbon dioxide [2]. Therefore, to meet the world's energy demand and mitigate climate change issues, the development of an alternative renewable and clean resource of energy is a prerequisite [3]. Plant biomass in the form of lignocellulosic biomass serves as a promising inexpensive feedstock for the production of biofuels such as bioethanol, biohydrogen, biomethanol, etc. to fuel the transportation sector [4–6]. Among these, presently, bioethanol is the

most common biofuel, owing to the transportation/storage and economical production constraints associated with biohydrogen and biomethanol, respectively [6]. Lignocellulosic biomass, such as forest materials and agro-industrial and municipal wastes, consist of an intricate network of biopolymers, such as cellulose, hemicellulose, and lignin [7]. The cellulose and hemicellulose fractions from the biomass can be hydrolyzed using cellulases and hemicellulases, respectively, into monomeric sugars, which are subsequently fermented to produce bioethanol [8]. The intense bonding between cellulose, hemicellulose, and lignin leads to biomass recalcitrance, which can be reduced by employing various pretreatment strategies, such as chemical, enzymatic, or microbial strategies [1]. Whole-cell-based cultures are also useful and economical for biomass treatment to release sugars [9]. While whole-cell-based cultures require nutrients and energy for growth and enzyme production, the enzymatic hydrolysis of cellulose is faster and yields more product than microbial action because it is a specific catalytic reaction that only needs ideal physical conditions (temperature, pH, and time) for efficient hydrolysis. Additionally, the product yield can also be enhanced by using purified enzymes, whereas whole-cell-based cultures may lead to the production of various unwanted enzymes/products, which may further interfere with the desired enzymatic hydrolysis reaction. The cellulase enzymes for industrial applications are naturally produced from various bacterial and fungal species on a large scale. However, the low concentrations, unfavorable conditions, specific substrate requirements, and high production cost, among others, are the few limitations associated with natural enzyme production [10]. Therefore, the focus has been shifted to the production of enzymes through recombinant technology using *Escherichia coli* as a host. Since *E. coli* can grow profusely on any growth medium, this approach offers the advantage of enabling the scaling up of the production of recombinant cellulase without the use of any particular substrates [10].

The production of cellulolytic enzymes for enzymatic hydrolysis in lignocellulosic biorefineries is a major bottleneck due to the high production cost of enzymes, which significantly impacts the cost-economics of biomass-to-biofuel conversion [5]. Furthermore, the high sensitivity of free enzymes, difficulty in separation from the reaction medium, non-reusability, and poor stability in extreme environmental conditions (temperature and pH) are several other hurdles that reduce the overall viability of the process. Consequently, the whole catalytic process is substantially hindered by their low operational stability, economic constraints, and short lifetime [11,12]. To overcome the aforementioned challenges and increase the enzyme's catalytic stability for the enzymatic saccharification of complex biopolymers such as cellulose and hemicellulose, enzyme immobilization appears to be a promising method [5]. Immobilization not only enhances enzyme stability in robust environments but also enables the recovery and reuse of enzymes for multiple cycles. This improves the overall process economy and efficient output in terms of high product yield [13]. Enzyme immobilization involves the binding or localization of enzymes onto a support surface or within a specific matrix. Immobilized enzymes replicate the natural mode of action and are more resistant to harsh milieu when they are bound to a support surface [14,15]. Enzyme immobilization can be achieved through physical interactions such as encapsulation and entrapment and chemical interactions such as covalent bonding, electrostatic interactions, hydrogen bonds, hydrophobic interactions, van der Waals interactions, and magnetic nanoparticles [5,12,16]. Enzymes immobilized via the covalent bond formation method can be used in reaction catalysis more frequently as it provides a more stable connection between the enzymes and support [12]. In this method, the surface of the carrier is first activated to produce functional groups (-COOH, -NH<sub>2</sub>, and -SH), which are then covalently linked with the enzyme using a cross-linker. Glutaraldehyde (GA) is used as a cross-linking reagent in covalent enzyme immobilization, which usually reacts with the amino group of the enzyme [17,18]. Moreover, it also prevents the leaching of the enzyme during recycling and maintains the robustness of the immobilized system [19]. Efficient enzyme immobilization is influenced by various factors, including the type of immobilization method and enzyme, immobilization conditions, enzyme loading, protein concentrations, etc. [20].

Enzyme purification is one of the crucial steps towards its biochemical and kinetic characterization for diverse industrial applications [21]. Moreover, the production of recombinant cellulases in *E. coli* also produces various unwanted proteins, making the purification of the protein a prerequisite [22]. Immobilized metal ion affinity chromatography (IMAC) has emerged as a well-accepted technology for protein purification from a bench scale to an industrial scale. Conventionally, it was based on the affinity of transition metal ions, such as Cu(II), Co(II), Fe(III), Zn(II), and Ni(II), towards histidine, tryptophan, and cysteine in aqueous solution, which was further extended to include the concept of using metal ions immobilized on a substrate to separate and purify proteins in liquids [23]. The interaction between an immobilized metal ion and electron donor groups on the surface of proteins forms chelated complexes that provide the basis for protein adsorption. The availability of histidine residues controls the actual protein binding in IMAC. The high specificity of IMAC is based on the difference between the strength of the various complexes formed [23]. The targeted protein can be eluted by using a low-pH buffer, a competitive displacement, or chelating agents.

The use of granular solid carriers in IMAC results in a pressure drop and often hinders the reaction. This shortcoming of IMAC can be overcome by using immobilized metal affinity membranes (IMAMs) [22]. This is the most widely used technique for the purification of proteins with mainly surface-exposed amino acids, such as histidine, tryptophan, cysteine, and tyrosine, or polyhistidine-tagged biomolecules [24,25]. Numerous membranes, viz., cellulose nitrate, regenerated cellulose (RC), and cellulose acetate, are used to prepare IMAMs; however, regenerated cellulose membranes (RCMs) offer various advantages, such as high hydrophilicity, chemical stability, biocompatibility, strong mechanical properties, and low non-specific adsorption [22]. Previously, our laboratory has purified penicillin G acylase using a modified RC-based IMAM technique. The membrane was successfully reused more than eight times after activation by regeneration [26].

Consequently, in the present study, the expression plasmid of endoglucanase (CelA) from the cellulosome of *Clostridium thermocellum* was constructed and expressed in *E. coli* and immobilized on a modified RC membrane. Two different membranes, i.e., IMAM (RC-EPI-IDA-Co<sup>2+</sup>; EPI, epichlorohydrin; IDA, iminodiacetic acid) for coordination coupling and the aldehyde functional group membrane (AM) RC-EPI-DA-GA (DA, 1,4-Diaminobutane) for covalent bonding, were prepared by subjecting the RC membranes to two different surface modifications. Moreover, the characterization of free and immobilized enzymes has been executed, and the difference in their kinetics is also discussed.

## 2. Results and Discussion

### 2.1. Cloning of Cellulase Gene in Plasmid

The cellulase gene CelA was inserted in plasmid pET21b to form the construct pET21b-CelA-his, which was further transformed into *E. coli* strains, namely, *E. coli* ER2566 and *E. coli* BL21. The plasmid was extracted and subjected to PCR and gene shearing. A clear band was visible after PCR, which is indicative of the presence of the target gene CelA fragment, with a molecular weight of 1.6 kb (Figure S1). Similar to the present study, the cellulase gene from *Bacillus subtilis* and *B. licheniformis* ATCC 14580 was cloned in *E. coli*, where the band appeared near 1.5 and 1.6 kb, respectively [10,27].

### 2.2. Recombinant Cellulase Expression under Different Conditions

#### 2.2.1. Effect of Different Hosts and Temperatures

After the pET21b-CelA-his plasmid was successfully transformed into *E. coli* ER2566 and *E. coli* BL21, protein expression analysis was carried out. The amount of protein expression is positively correlated with temperature, as the higher the temperature, the shorter the incubation time and the faster the protein expression. However, an induction at higher temperatures may result in the formation of the insoluble proteinaceous matter known as inclusion bodies, which blocks protein translocation and cannot be used [28]. In the current study, the induction was set at 15 °C for 24 h and at 37 °C for 6 h to observe

the performance of the target protein at different induction temperatures and times. The protein expression was confirmed by the presence of a bright band after sodium dodecyl sulfate polyacrylamide gel electrophoresis (SDS-PAGE) of the target protein of a molecular weight of about 60 kDa, irrespective of the host and culture conditions used (Figure 1a). The integrated color intensity of each band was calculated by ImageJ software to quantify the target protein (Figure 1b). The results indicated that the maximum amount of protein was obtained when *E. coli* ER2566 was used as the expression host under the culture condition of 37 °C for 6 h. Therefore, *E. coli* ER2566 was used as the expression host in subsequent experiments and was induced and cultured at 37 °C for 6 h.

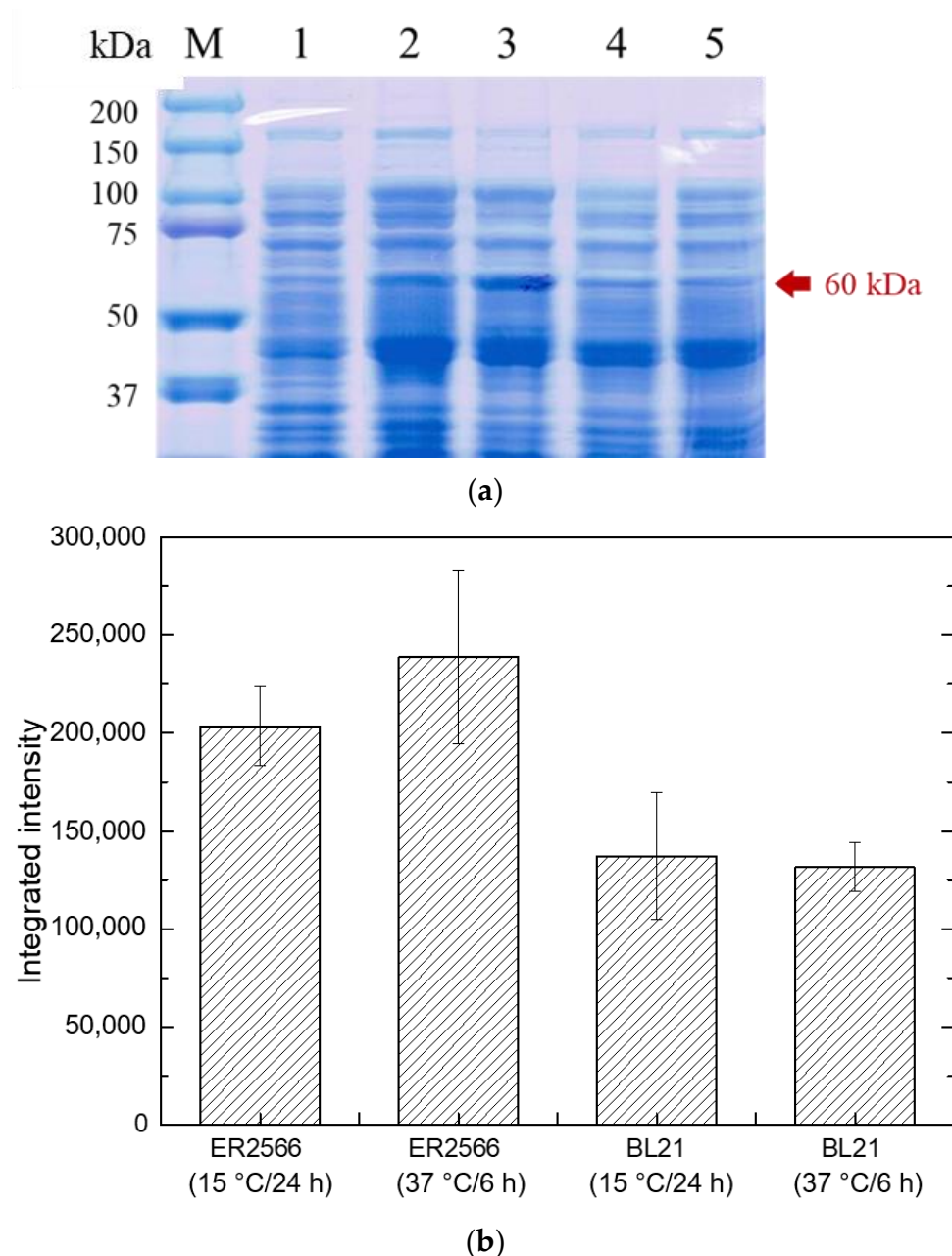


**Figure 1.** (a) SDS-PAGE electropherogram of pET21b-CelA-his with different hosts and temperatures. Lane M: marker (kDa); Lane 1: pET21b; Lane 2: pET21b-CelA-his/ER2566 (15 °C/24 h); Lane 3: pET21b-CelA-his/ER2566 (37 °C/6 h); Lane 4: pET21b-CelA-his/BL21 (15 °C/24 h); Lane 5: pET21b-CelA-his/BL21 (37 °C/6 h). (b) ImageJ analysis of protein content of pET21b-CelA-his in different hosts and temperatures.

### 2.2.2. Effect of Different Inducer Concentrations

The production of recombinant proteins in *E. coli* has been extensively carried out using a T7-promoter-based expression system, with isopropyl  $\beta$ -D-1-thiogalactopyranoside (IPTG) as an inducer [28]. Recombinant protein expression is greatly influenced by the concentration and timing of the addition of the inducer IPTG. Higher concentrations of IPTG, apart from impacting the cost-economics of the process, may cause cell toxicity, whereas lower concentrations result in inadequate protein induction, thus, reducing the efficiency. Therefore, the regulation of IPTG concentration is vital for successful protein expression [29]. In this study, different IPTG concentrations, viz., 0.1, 0.3, 0.5, and 0.7 mM were used. A sharp band of the target protein of molecular weight 60 kDa was observed after induction, which indicated that a higher amount of target protein was produced after induction compared to without induction (Figure 2a). At the IPTG concentration of 0.1 mM, the sharpest and brightest band was observed. The amount of target protein was estimated by determining the integrated color intensity of each band by using ImageJ software (Figure 2b). Therefore, IPTG was used at the 0.1 mM concentration as the inducer in subsequent experiments. In another research work, Mühlmann et al. demonstrated the relationship between inducer concentration and induction temperature and time on the metabolic state of *E. coli*. and the formation of the product. Their results exhibited a decrease in the optimal inducer concentration to 0.05 mM IPTG from 0.1 mM IPTG at 28 °C and at elevated temperatures (34 and 37 °C) [30]. These findings indicate that lower IPTG concentrations are favorable at higher temperatures.

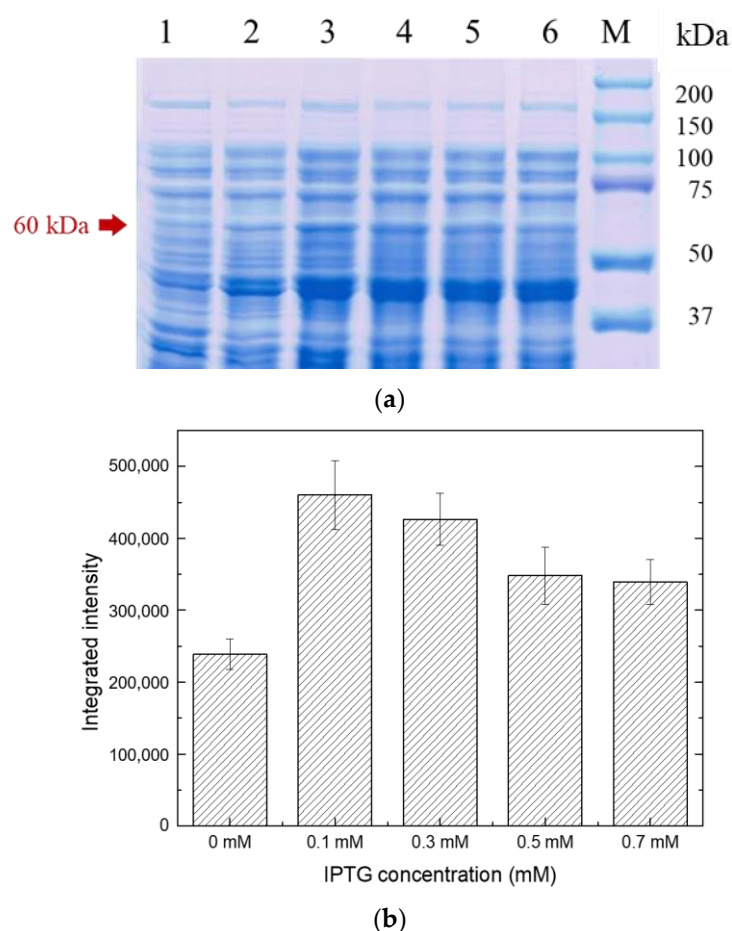
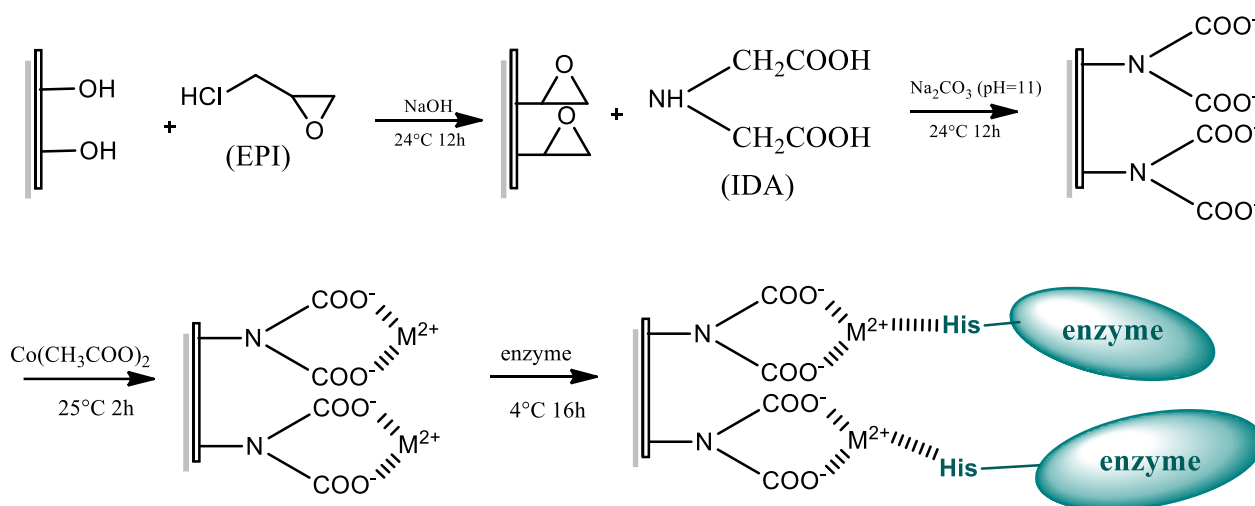


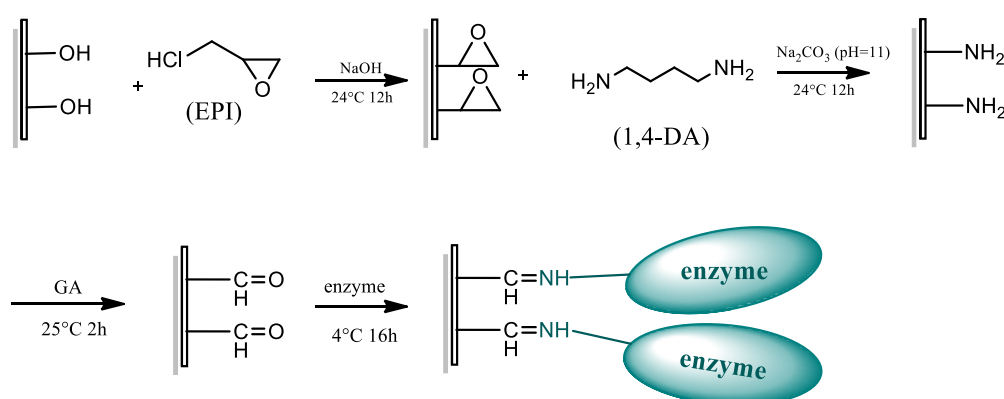
**Figure 2.** (a) SDS-PAGE electrophoresis of recombinant protein induced by different IPTG concentrations. Lane M: marker (kDa); Lane 1: pET21b; Lane 2: not induced; Lane 3: 0.1 mM; Lane 4: 0.3 mM; Lane 5: 0.5 mM; Lane 6: 0.7 mM. (b) ImageJ analysis of the protein amount induced by different IPTG concentrations.

### 2.3. Characterization of Modified RC Membranes

The RC membrane used in this study is reinforced with nonwoven cellulose, which has been tested not to be digested by CelA prior to immobilization experiments. The preparation steps of RC-EPI-IDA and RC-EPI-DA-GA membranes for CelA immobilization are shown in Schemes 1 and 2. The Fourier-transformed infrared spectroscopy (FTIR) analysis was performed after the surface modification of RC membranes to understand the functional group changes that occurred in membranes post-modification in contrast to RC membranes without modifications. Figure 3a shows the FTIR spectra of the RC membrane and the RC-EPI-IDA membrane after surface modification with EPI and IDA (before metal chelation). The intensity of absorption peak at  $901\text{ cm}^{-1}$  for the OH group in the unmodified RC membrane was reduced in the modified RC membrane, indicating the activation of the membrane by EPI [31]. The characteristic absorption peak of the epoxy group in the range of  $950\text{ to }815\text{ cm}^{-1}$  in the spectrum of the EPI-activated RC membrane was observed [31]. After adding IDA, the absorption peaks at  $1774\text{ and }1196\text{ cm}^{-1}$  for the carboxylate group were visible [31]. The peaks for the C-N and C=O groups of IDA were also observed at  $1368\text{ and }1680\text{ cm}^{-1}$ , respectively, confirming the successful modification of the surface of the RC membrane by EPI and IDA.



**Scheme 1.** RC-EPI-IDA membrane preparation.



**Scheme 2.** RC-EPI-DA-GA membrane preparation.

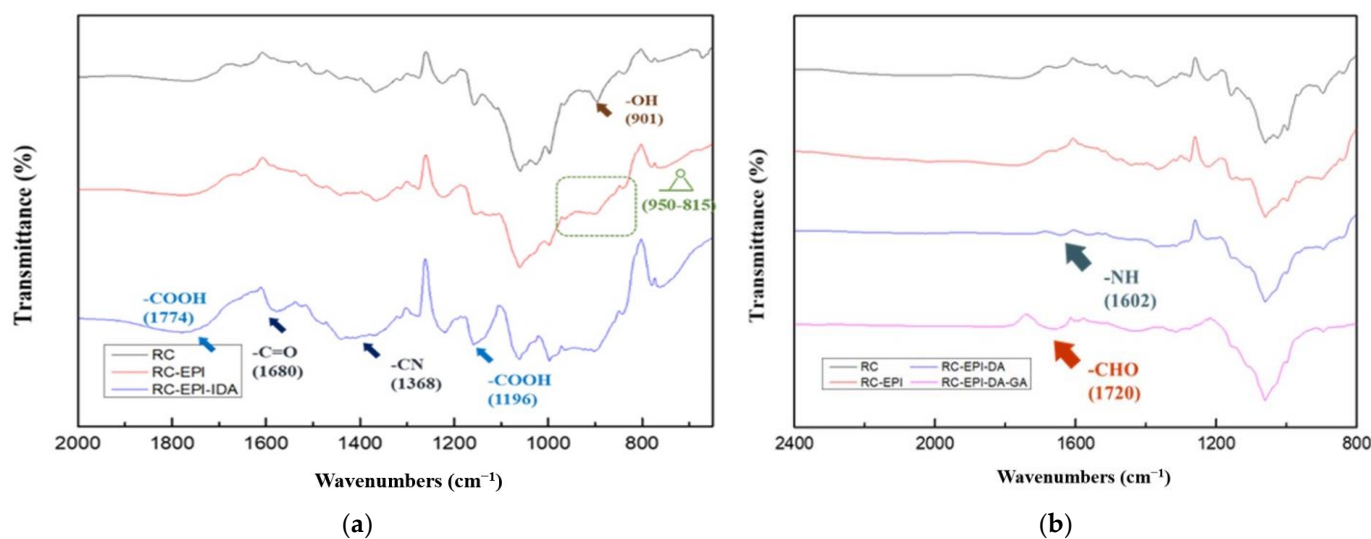


**Figure 3.** FTIR characterization of (a) RC-EPI-IDA membrane and (b) RC-EPI-DA-GA membrane.

Figure 3b shows the FTIR spectra of the RC membrane and the RC-EPI-DA-GA membrane after surface modification with 1,4-DA and GA. Modification by 1,4-DA was confirmed by the presence of an absorption band at  $1602\text{ cm}^{-1}$ , corresponding to N-H bending in 1,4-DA [32]. A peak at  $1720\text{ cm}^{-1}$ , representing the free aldehyde group of GA, confirmed the successful membrane activation by GA [33].

#### 2.4. Metal Ion Selection for IMAM Chelation and Effect on Enzyme Activity

In order to couple metal ions with the modified membrane RC-EPI-IDA, first, the effect of metal ions on the activity of free enzyme Cella must be determined. Therefore, the effect of various metal ions, viz.,  $\text{Zn}^{2+}$ ,  $\text{Al}^{3+}$ ,  $\text{Cu}^{2+}$ ,  $\text{Ni}^{2+}$ ,  $\text{Fe}^{3+}$ ,  $\text{Mn}^{2+}$ , and  $\text{Co}^{2+}$ , on the activity of free Cella enzymes was studied. The initial activity of the free enzymes was  $1.25\text{ U/mL}$ , which was taken as control (100%). The  $\text{Zn}^{2+}$ ,  $\text{Al}^{3+}$ ,  $\text{Cu}^{2+}$ , and  $\text{Ni}^{2+}$  metal ion solutions exhibited an inhibitory effect on the endoglucanase activity. However, the Cella endoglucanase activity was improved in the  $\text{Fe}^{3+}$ ,  $\text{Mn}^{2+}$ , and  $\text{Co}^{2+}$  metal ion solutions (Figure S2). Metal ions facilitate the binding of enzymes to the substrate to enhance enzymatic action by activating electrophiles or nucleophiles via electron transfer reactions. Metal ions may also help in maintaining three-dimensional active confirmation by bringing the enzymes and substrate into close proximity via a coordinate [21]. However, the enzyme-substrate complex may sometimes be broken up by metal ions action, changing the proper interactions between the substrate and the enzyme and resulting in a loss of activity [21]. The metal ions  $\text{Mn}^{2+}$  and  $\text{Co}^{2+}$  have been reported to improve the hydrolysis activity of endoglucanase in the literature. CTendo7's endoglucanase activity was increased in the presence of  $\text{Mn}^{2+}$  and  $\text{Co}^{2+}$ , which are heterologously expressed in *Pichia pastoris* [34].

The amount and activity of the adsorbed protein were measured to calculate the specific activity of the enzyme after the chelation of different metal ions on IMAM and enzyme immobilization. The results indicated that IMAMs with  $\text{Cu}^{2+}$  on chelation were able to adsorb the most amount of protein, but the specific activity ( $0.80\text{ U mg}^{-1}$ ) was lower than in other metal ions, which might be due to inhibition of Cella endoglucanase by  $\text{Cu}^{2+}$  (Figure 4).  $\text{Cu}^{2+}$  is known for its inhibitory effect on many glycoside hydrolases due to the auto-oxidation of proximal cysteine residues, which results in the formation of inter- and intra-molecular disulfide bridges [34]. The amount of protein adsorbed by other metal ions was almost similar; however,  $\text{Co}^{2+}$  and  $\text{Mn}^{2+}$  significantly increased the endoglucanase activity, which further resulted in high specific activity ( $2.07$  and  $2.00\text{ U mg}^{-1}$ ) in the case of these two metal ions (Figure 4). Therefore, the IMAMs coupled with  $\text{Co}^{2+}$  and  $\text{Mn}^{2+}$  were further analyzed to check their reuse ability. It was observed that the activity of the IMAM- $\text{Mn}^{2+}$  immobilized enzyme decreased very quickly after several repeated uses

(Figure 5).  $\text{Co}^{2+}$ , being an intermediate metal ion, tends to form a covalent bond with oxygen, sulfur, nitrogen, and histidine and, thus, may improve the catalytic efficiency of the enzyme [35]. Therefore,  $\text{Co}^{2+}$  was used for the chelation of IMAMs in the subsequent experiments. The chelation was executed with 50 mM cobalt ion solution for 3 h, and the immobilized enzyme was referred to as RC-EPI-IDA- $\text{Co}^{2+}$ -CelA. IMAMs chelated with  $\text{Co}^{2+}$  have been used for the simultaneous purification and immobilization of the xylanase enzyme, which is heterologously expressed in *E. coli*. The presence of  $\text{Co}^{2+}$  metal ions increased the activity of both free and immobilized enzymes [22].

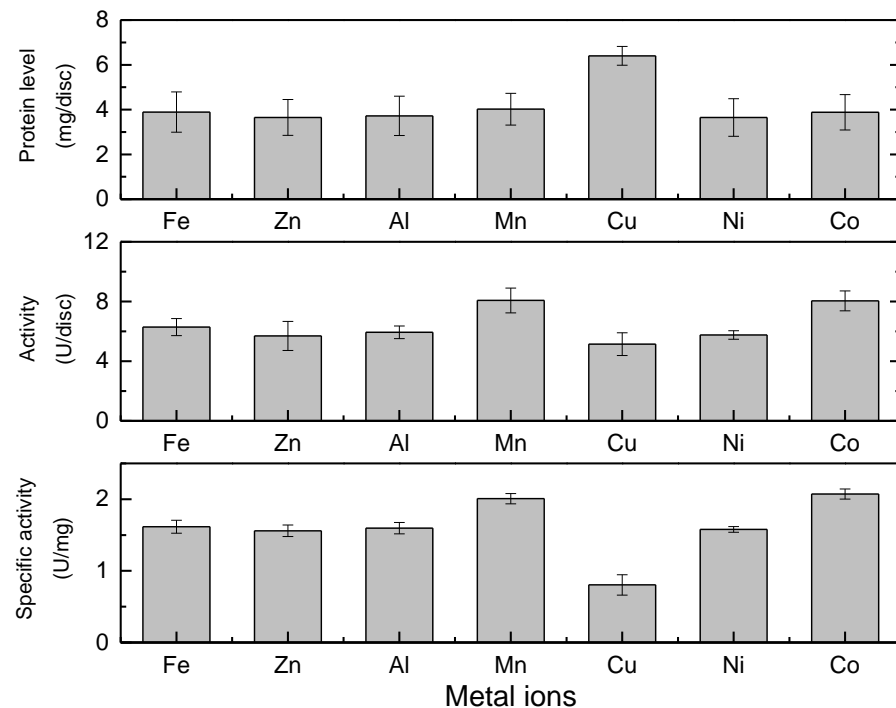


**Figure 4.** Protein adsorption capacity, activity, and specific activity of IMAMs chelated with different metal ions on CelA.

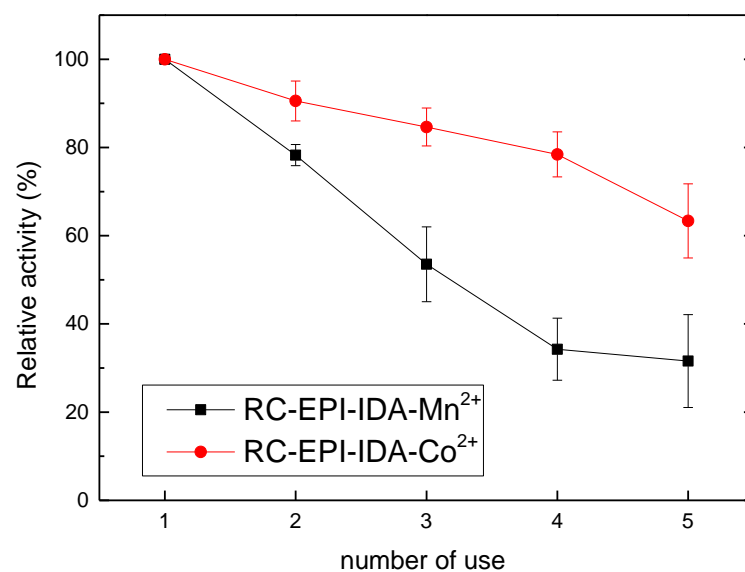


**Figure 5.** Reusability of immobilized enzymes using IMAM- $\text{Co}^{2+}$  and IMAM- $\text{Mn}^{2+}$ .

### 2.5. Effect of GA Concentration and Treatment Time

The enzyme immobilization was also executed using an RC-EPI-DA-GA membrane, wherein GA was used as an activator, and the immobilized enzyme was referred to as RC-EPI-DA-GA-CelA. GA, a bi-functional chemical, condenses aldehyde on the surface of the RC membrane to produce active  $\alpha$ ,  $\beta$ -unsaturated aldehyde, which subsequently binds to an amino group of protein, resulting in the formation of a complex and stable product via covalent bonding [18]. The immobilization of the enzyme is greatly influenced by GA concentration and the duration of its treatment. Therefore, in the current study, GA concentration (0.05, 0.1, 0.2, 0.5, and 1%, *v/v*) and its treatment time (1–5 h) were optimized to evaluate the effect on enzyme activity. It was observed that at the GA concentration of 0.5% (*v/v*), the maximum amount of protein immobilization occurred. However, the maximum CelA endoglucanase activity of 8.1 U was obtained at 0.1% (*v/v*) GA concentration, which was reduced at 0.2% (*v/v*) (Figure 6). The decrease in CelA endoglucanase activity at higher GA concentrations is attributed to the fact that higher GA concentrations alter the enzyme conformation since it is a protein denaturant and also increase the rigidity of the enzyme because of too much cross-linking, which reduces enzyme activity [18,36]. Moreover, insufficient endoglucanase-GA cross-linking may also cause the activity to decline at lower GA concentrations [36].

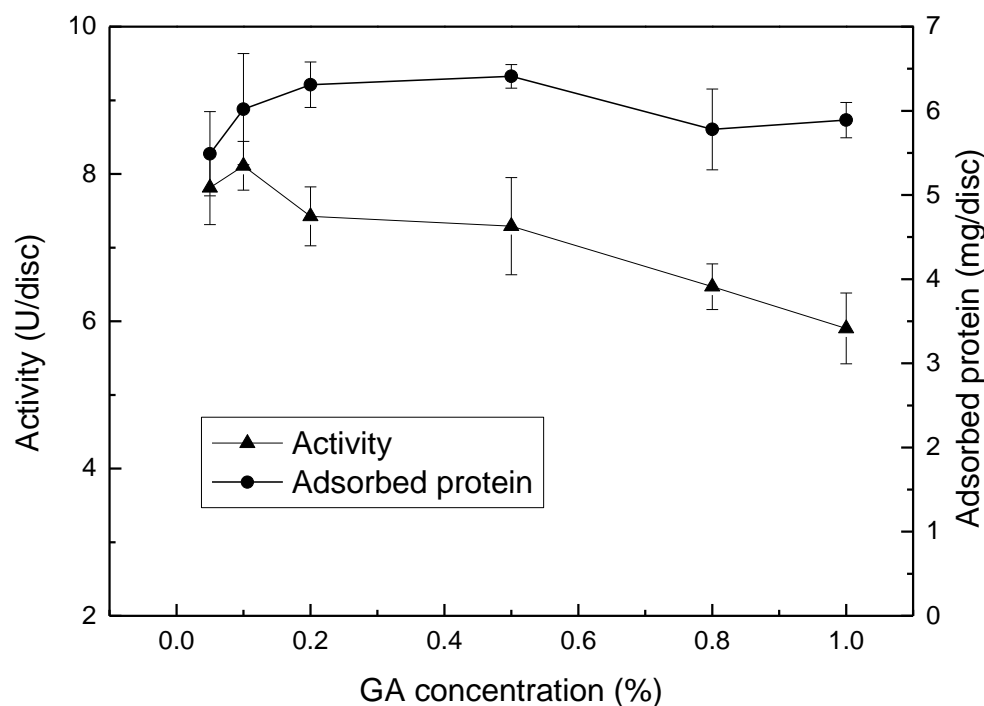


**Figure 6.** Effect of different concentrations of GA on CelA endoglucanase activity, and protein adsorption.

In the case of GA treatment time with RC-EPI-DA, the maximum CelA endoglucanase activity was found at 2 h of treatment time. A reduction in CelA endoglucanase activity was seen when the treatment time was 4 h (Figure S3). The optimization of GA treatment time is crucial for efficient enzyme activity as the longer duration of treatment may result in interactions at multiple sites on the carrier, thereby reducing the number of sites for enzyme immobilization, whereas shorter treatment time may not be sufficient to completely activate the functional groups on the matrix for enzyme immobilization, leading to reduced activity [18]. Therefore, in the subsequent experiments, the GA treatment was carried out for 2 h at a concentration of 0.1% (*v/v*). There are many reported studies wherein GA has been used as a cross-linking agent, and emphasis has been laid on the impact of GA concentration and treatment time. In a study, cross-linked cellulase aggregates (C-CLEAs) were synthesized, and GA was used as a cross-linker. The concentrations of GA and cross-

linking time were optimized, and the maximum cellulase activity was achieved at 2% (*v/v*) concentration with 3.5 h of cross-linking time [37]. Similarly, the maximum activity of the inulinase enzyme was observed at 1.59% concentration and the treatment time of 4 h [18].

### 2.6. Purification Analysis

For a thorough examination of the catalytic, kinetic, structural, and functional properties of enzymes, enzyme purification is considered a crucial step [21]. Therefore, the purification efficiency achieved from the immobilization of enzymes on two different membranes was estimated. A 3.192 and 1.536 purification fold was achieved with RC-EPI-IDA-Co<sup>2+</sup>-CelA and RC-EPI-DA-GA-CelA, respectively (Table 1). A single band of purified CelA was obtained on SDS-PAGE (Figure S4). The CelA endoglucanase enzyme contained His-tag, which could bind more strongly to the IMAM membrane because of an affinity for Co<sup>2+</sup> metal ions and, therefore, result in the high purification of the enzyme [23]. IMAMs have been used for the purification of His-tagged recombinant serine hydroxymethyl transferase using various metal ions, and 5-fold purification has been achieved with Co<sup>2+</sup> ions [37].

**Table 1.** Activity and purification effect of free and immobilized enzymes.

Sample	Activity (U/mL or U/disc)	Protein (mg/mL)	Specific Activity (U/mg)	Purification Fold
Free CelA <sup>a</sup>	1.250	1.322	0.946	1.00
RC-EPI-IDA-Co <sup>2+</sup> -CelA <sup>b</sup>	9.42	3.12	3.02	3.19
RC-EPI-DA-GA-CelA <sup>b</sup>	7.24	4.98	1.45	1.54

<sup>a</sup> activity expressed in U/mL; <sup>b</sup> activity expressed in U/disc.

### 2.7. Optimal pH and Enzyme Stability

Any industrially significant enzyme must be able to maintain its catalytic activity and stability in extreme pH environments. In acidic or alkaline pH, the ionic group of the enzyme shows varying degrees of protonation, which result in a change in enzyme configuration and, ultimately, affect enzyme activity [22]. In our present study, the effect of different pH levels and the pH stability of free enzymes and immobilized CelA endoglucanase was studied. The maximum activity (100%) of free enzymes was obtained at optimal pH 5, which increased to pH 6 (100%) for RC-EPI-IDA-Co<sup>2+</sup>-CelA and RC-EPI-DA-GA-CelA enzymes (Figure 7a). The activity of free enzymes decreased at pH 6; however, immobilized enzymes demonstrated high relative activity (80–60%) over a broad pH range (pH 4–9). The high activity retention of immobilized enzymes in a wide pH range may be attributed to the stable rigidity and confirmation of the enzyme provided by multipoint attachment due to interaction between the charged groups of the enzyme and carrier [38,39]. The results were aligned with previously reported studies. The optimal pH value of the endoglucanase of *Arachniotus citrinus* was increased from 4.9 to 5.6 after immobilization on polyacrylamide gel [40]. Similarly, cellulase immobilization on sodium alginate-polyethylene glycol showed maximum activity at the optimal pH value of 5, whereas for free cellulase, the optimal pH was 4 [41]. The current and previous findings indicate that cellulase shows proficient activity in the pH range of 4–6.

The stability of free enzymes and immobilized CelA endoglucanase at varying pH ranges was also analyzed, as the enzyme activity is highly influenced by its storage environment. The enzyme was exposed to various pH values for 2 h at 4 °C. The initial enzyme activity was taken as 100%. It was observed that the stability trend for free and immobilized enzymes over a pH range of 4–9 was similar, and enzymes exhibited approximately 80% relative activity in both free and immobilized forms (Figure 7b). It was evident from the results that immobilization did not lead to any change in the confirmation of CelA endoglucanase, and it was able to retain active three-dimensional orientation, indicated by efficient catalytic activity. The stability of free or immobilized enzymes at a wide pH range also exhibited its potential for industrial applications.

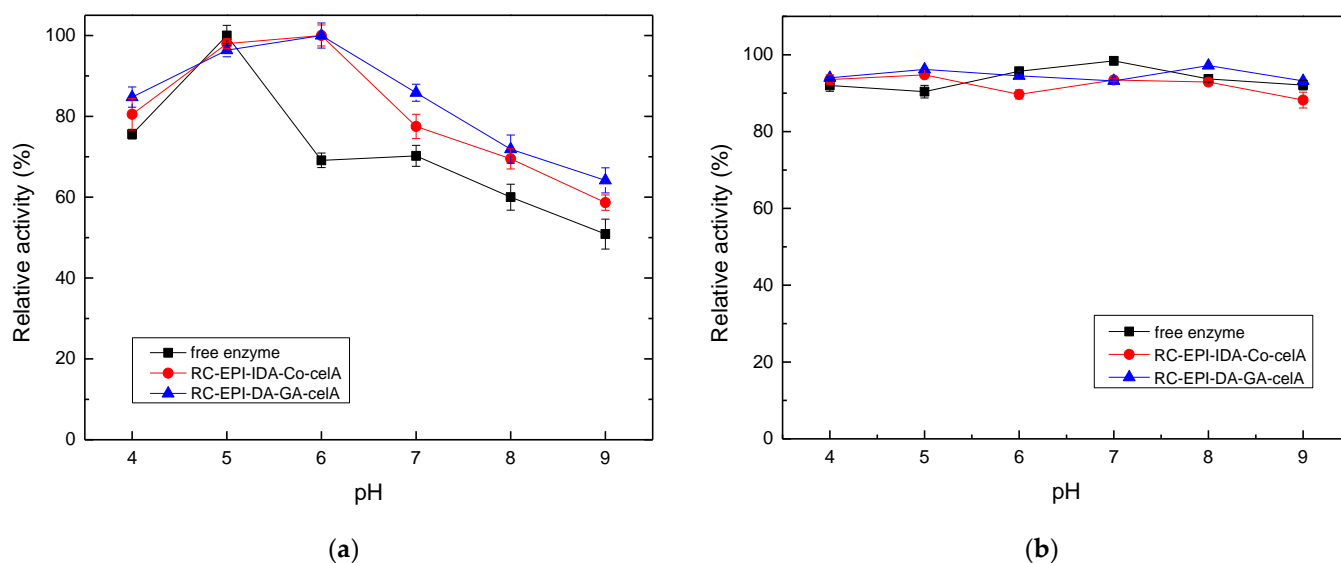


**Figure 7.** (a) Optimum pH and (b) pH stability of free and immobilized CelA endoglucanase.

### 2.8. Optimal Temperature and Thermo-Stability

Enzyme stability at extreme temperatures is also very crucial for industrial potential. High temperatures increase the rate of reaction by increasing the rate of effective collision between molecules. However, in an enzymatic reaction at a high temperature, the catalytic efficiency of the enzyme is reduced as the elevated temperature leads to changes in the active structure of the enzyme. Therefore, the optimal temperature and thermo-stability of free and immobilized enzymes were investigated. It was observed that the relative activity of the immobilized enzyme was higher compared to the free enzyme over a temperature range of 50–80 °C, with a temperature optima of 60 °C for free and RC-EPI-IDA-Co<sup>2+</sup>-CelA enzymes and 70 °C for the RC-EPI-DA-GA-CelA enzyme (Figure 8a). The increase in optimal temperature for the RC-EPI-DA-GA-CelA enzyme could be explained by a decrease in the flexibility of the enzymes on a solid matrix, resulting in improved tolerance to unfolding and denaturation owing to conformational changes [39]. The results were inconsistent with previous studies, where the optimum temperature for free and immobilized cellulase is reported to be between 50–70 °C [39,41]. The temperature optima of cellulase enzyme from *Aspergillus fumigatus* immobilized on magnetic nanoparticles was 60 and 50 °C for free enzymes [39]. Likewise, the immobilization of cellulase on sodium alginate-polyethylene glycol resulted in an increased optimal temperature (70 °C) compared to free enzymes (50 °C) [41]. Therefore, the findings from this study and the literature substantiate that the optimal temperature falls within the range of 50–70 °C.

The thermal stability of enzymes is a crucial characteristic since enzyme activity can be affected by the extreme temperatures employed in various industrial processes. Therefore, the thermo-stability of free and immobilized CelA endoglucanases was also evaluated. The free and immobilized CelA endoglucanases were incubated at different temperatures (50–90 °C) for 1 h, and then, activity was measured. Figure 8b reveals that both the free enzyme and the immobilized enzyme exhibit 85% relative activity within a temperature range of 50–70 °C. The enzyme activity of the free enzymes drastically declined at 80 and at 90 °C, and the free enzyme relative activity decreased to 20%. However, in the case of immobilized enzymes, even though the reduction in activity was seen after 80 °C, the RC-EPI-IDA-Co<sup>2+</sup>-CelA-immobilized enzymes retained 54% of the initial activity, and RC-EPI-DA-GA-CelA also retained 65% of the initial activity. The higher thermo-stability of the immobilized enzyme might be due to the more stable spatial configuration of the enzyme due to immobilization [41]. Thus, it was evident that the two immobilization methods made the enzyme more resistant to high temperatures and increased thermal stability over a wider temperature range.

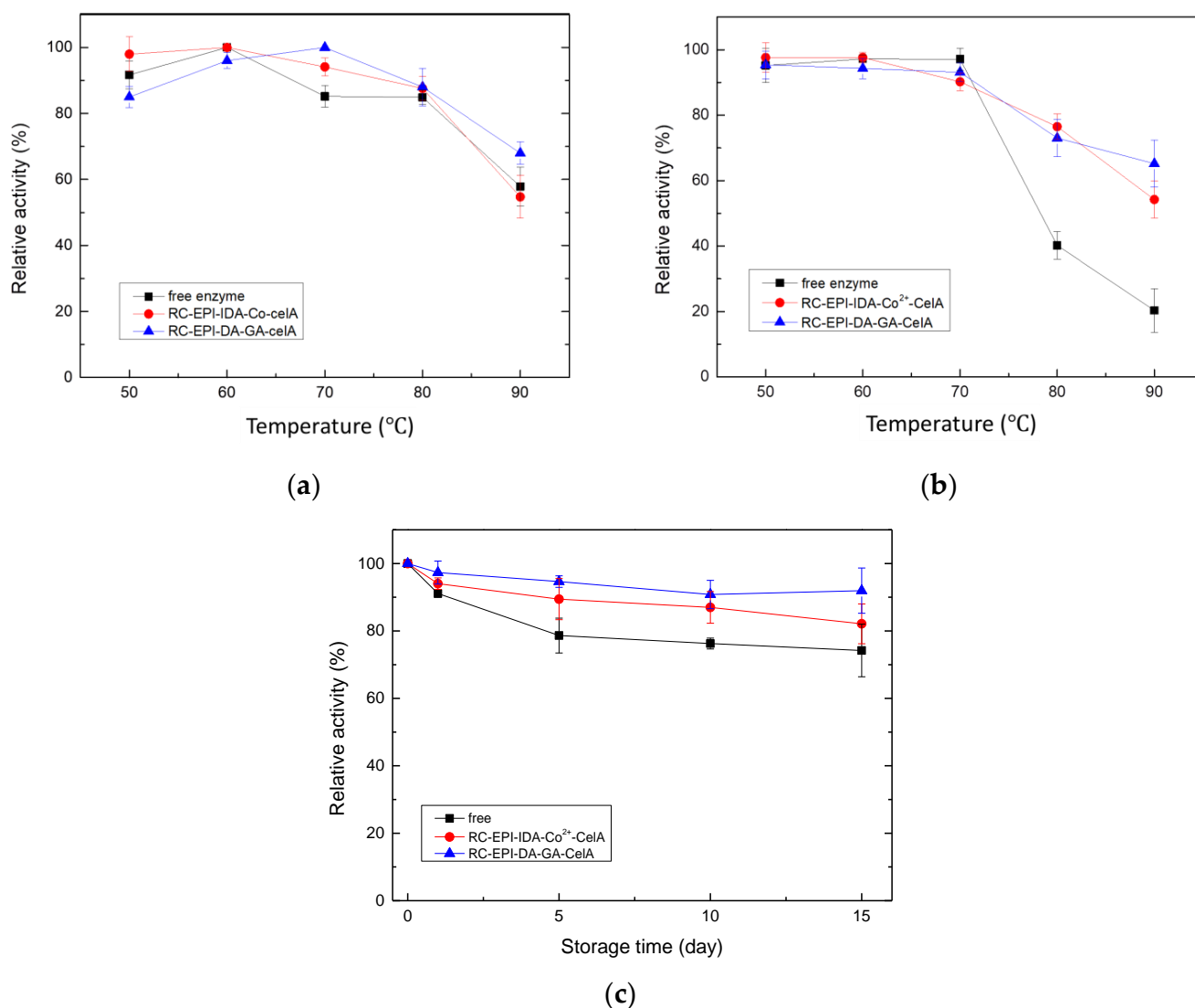


**Figure 8.** (a) Optimum temperature, (b) thermo-stability, and (c) storage stability of free and immobilized CelA endoglucanase.

The free and immobilized enzymes were analyzed for their storage stability at 4 °C for 5, 10, and 15 days. The activity on the 0th day was considered as the initial activity. Figure 8c reveals that RC-EPI-DA-GA-CelA maintained the best relative activity within 15 days, followed by RC-EPI-IDA-Co<sup>2+</sup>-CelA. Both immobilization methods showed better preservation compared with free enzymes, retaining 91% and 82% of their relative activities after 15 days, respectively (Figure 8c). The results indicated that immobilization increased the shelf life of an enzyme [42]. The increased stability at 4 °C could be attributed to the rigidity and decreased flexibility of enzymes due to immobilization.

### 2.9. Enzyme Reusability Analysis

The most important advantage of enzyme immobilization is the ability to reuse the enzymes. The reusability of enzymes is a decisive factor that significantly governs the techno-economically viability of any enzyme-driven process. Therefore, under the optimized conditions discussed in the above experiments, the activity of both membranes was repeatedly investigated (five times) to determine the change in relative activity after multiple uses. The results revealed that 63% and 53% of the relative activity was retained for RC-EPI-IDA-Co<sup>2+</sup>-CelA and RC-EPI-DA-GA-CelA, respectively, after five times of reuse (Figure 9). The loss of relative activity could be attributed to inadequate binding be-

tween the enzyme and the support [43]. In previously reported studies, chitosan–cellulase nanomixtures immobilized in alginate beads retained only 18% activity after five cycles of reuse [43], whereas 59.42% enzyme relative activity was observed after five cycles when the cellulase was immobilized on sodium alginate-polyethylene glycol-chitosan [44]. Therefore, it can be concluded that the immobilization of enzymes on RC-EPI-IDA-Co and RC-EPI-DA-GA is economically beneficial for the process as the membranes can be reused multiple times and retain sufficient enzyme activity.

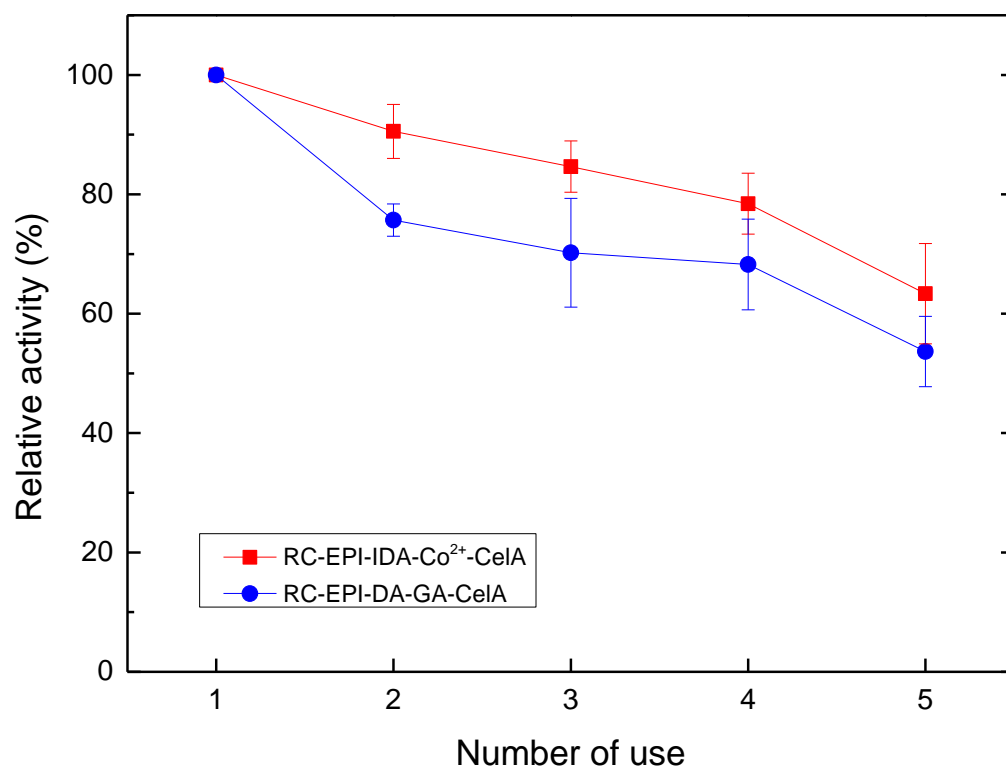


**Figure 9.** Reusability of RC-EPI-IDA-Co<sup>2+</sup>-CelA and RC-EPI-DA-GA-CelA enzymes.

### 2.10. Kinetics Study of Free and Immobilized Enzymes

A kinetic parameter analysis of free and immobilized enzymes was carried out to study the catalytic rate of enzyme-catalyzed reactions. Free and immobilized enzyme activity was assayed at different substrate concentrations to determine  $K_m$  (Michaelis–Menton constant) and  $V_{max}$  (maximal velocity). The behavior of enzymes is best described by enzyme kinetic constants, i.e.,  $K_m$  and  $V_{max}$ , which are dependent on varying concentrations of the substrate [45].  $K_m$  defines the affinity of an enzyme towards a substrate. A lower  $K_m$  value indicates the higher affinity of an enzyme to its substrate and vice versa.  $V_{max}$  denotes a maximum rate of enzyme-catalyzed reaction when a substrate is converted into a product under specific conditions [46]. The Lineweaver Burk plot, depicted in Figure 10, shows a straight line between substrate concentrations ( $1/[S]$ ) and reaction velocity ( $1/[V]$ ). The  $K_m$  and  $V_{max}$  of free and immobilized enzymes were determined by analyzing the intercepts on the X- and Y-axes of the double reciprocal plot. The results revealed that immobilized enzymes have better  $V_{max}$  and  $K_m$  compared to free enzymes (Table 2). Among all enzymes, the RC-EPI-IDA-Co<sup>2+</sup>-CelA enzyme had the lowest  $K_m$  value, which indicated its maximum affinity for the substrate, followed by RC-EPI-DA-GA-CelA, and then the free enzyme. Similar trends of results were found in the case of the  $V_{max}$  value. The decrease in the  $K_m$  value and the increase in the  $V_{max}$  value of immobilized enzymes compared to free enzymes could be attributed to the structural changes that occurred in the enzyme due to immobilization [47]. Moreover, it is speculated that the immobilized enzyme has the effect of preliminary purification due to IMAM immobilization, which

eliminates protein impurities, lowers hindrances between the enzyme and the matrix, and increases affinity. Additionally, as described in Section 2.4, the cobalt ions can boost the activity of CelA endoglucanase, thereby increasing the maximal reaction rate and  $V_{\max}$  and making the immobilization approach of IMAMs more effective. The results are consistent with other studies, wherein the decrease in  $K_m$  and increase in  $V_{\max}$  values have been reported for different enzymes immobilized using IMAM/IMAC [47,48]. In our previous study, the  $K_m$  value of xylanase immobilized on IMAMs decreased compared to free enzymes (8.445 mg/mL), with a minimum  $K_m$  of 1.513 mg/mL for IMAM- $\text{Co}^{2+}$ -CipA-XynCt. Similarly, a maximum  $V_{\max}$  of 3.831 U/mg was achieved for IMAM- $\text{Co}^{2+}$ -CipA-XynCt compared to free enzymes (2.235 U/mg) [22].

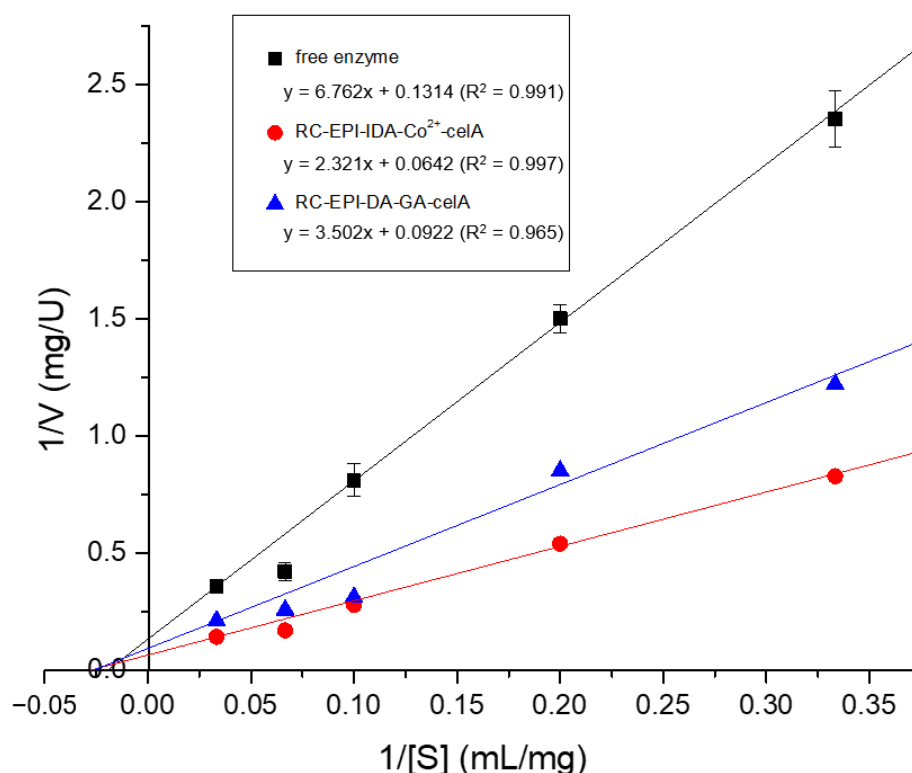


**Figure 10.** Lineweaver Burk plot mapping of free and immobilized CelA endoglucanase.

**Table 2.** Kinetic parameters of free and immobilized CelA endoglucanase.

Enzymes	$V_{\max}$ (U/mg)	$K_m$ (mg/mL)
Free enzyme	7.61	51.45
RC-EPI-IDA- $\text{Co}^{2+}$ -CelA	15.57	36.14
RC-EPI-DA-GA-CelA	10.85	37.99

### 2.11. Regeneration of IMAM

The IMAM prepared in this study was a reversible immobilized membrane, and the catalytic activity of the enzyme immobilized on the membrane decreased with multiple uses over a longer period of time. Thus, the regeneration of enzyme-immobilized IMAMs is important, wherein the enzyme and metal ions are desorbed and re-adsorbed again. There are two proposed approaches commonly applied to regenerate membranes. The use of imidazole is the most common way to desorb the His-tag target protein in many purification processes, while the use of ethylenediaminetetraacetic acid (EDTA) can desorb not only protein but also the chelated metal ion [49]. It can be seen in Figure 11 that the use of 250 mM imidazole resulted in a drop in relative activity to 38.4% of the original after five times of regeneration, while with the use of 100 mM EDTA to desorb metal ion, a relative activity of

51.2% was obtained after five times of regeneration. It is proposed that when the metal ion membrane is regenerated using the imidazole of EDTA, a thin layer of precipitate is formed on the IMAM membrane surface. These precipitates are mainly the cell debris and non-specific protein present in the crude enzyme extract, which adsorbs to the membrane surface. Although these precipitates do not interfere with metal ion adsorption, they, however, affect the adsorption capacity of the enzyme due to steric hindrance, resulting in lower enzyme activity [49]. Therefore, in the regeneration process, various other stripping solutions, alone or in combination, including EDTA, hydrochloric acid (HCl), sodium hydroxide (NaOH), and binding buffer, were investigated for the removal of precipitated contaminants.

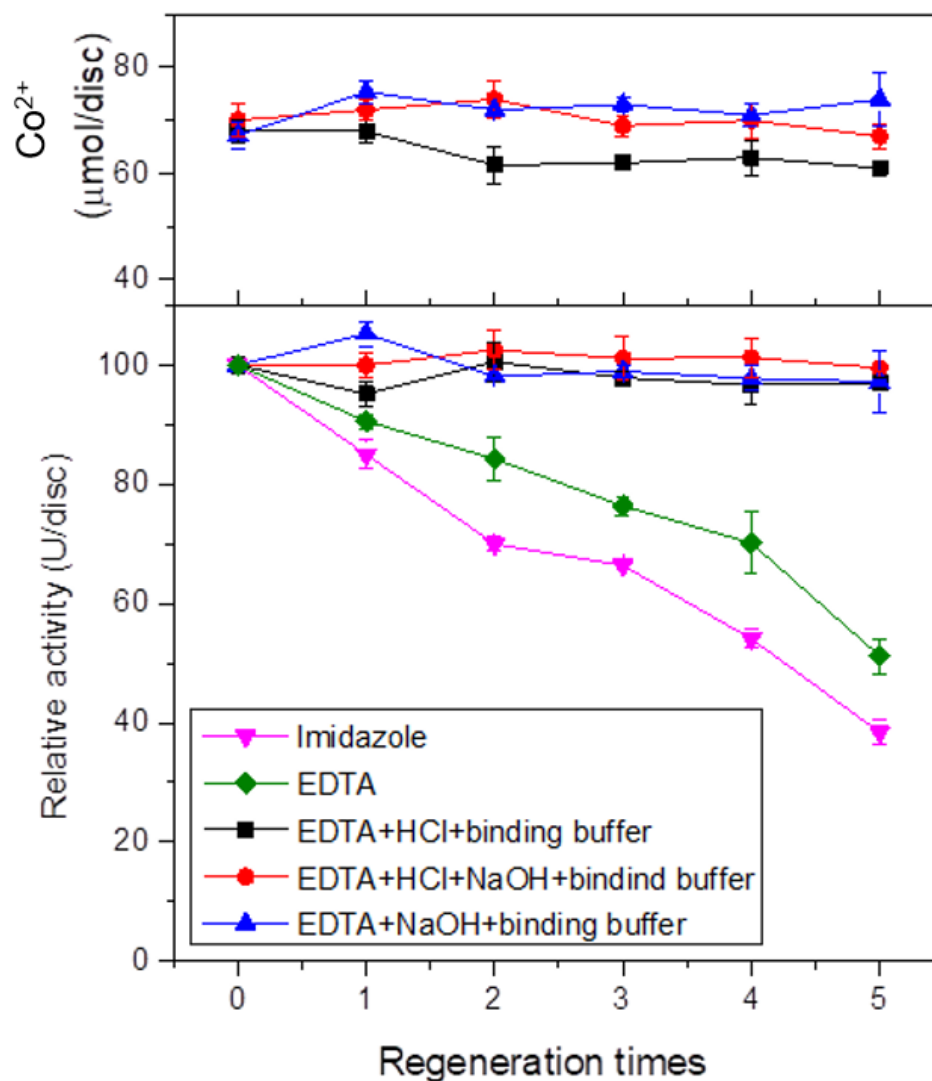


**Figure 11.** Impact of various stripping solutions on IMAM regeneration.

The combination of HCl or/and NaOH with EDTA sequentially in binding buffer as a stripping solution resulted in almost the same levels of metal ion and protein adsorption in the regenerated membrane (Figure 11). In addition, the adsorbed CelA endoglucanase activity after each regeneration process was almost similar to the original activity. This indicated that the proposed regeneration methods, by the addition of either HCl or NaOH, can effectively remove the impurity contaminants on the surface of IMAMs to regenerate a new IMAM for effective CelA coupling. This is the first report on developing and using reversible IMAMs as a matrix for recombinant endoglucanase immobilization.

### 3. Materials and Methods

#### 3.1. Chemicals, *E. coli* Strains, and Plasmid Sources

The chemicals used in the study were purchased from Showa (Gunma, Japan), BD Biosciences (San Jose, CA, USA), Amresco (Solon, OH, USA), Fisher Scientific (San Jose, CA, USA), Sartorius (Göttingen, Germany), Sigma (St. Louis, MO, USA), BIO-RAD (Hercules, CA, USA), and Alfa Aesar (Karlsruhe, Germany) and were of analytical grade. An RC disc film, procured from Sartorius Stedim Biotech, was used as the solidified carrier, with a diameter of 4.7 cm and a pore size of 0.45  $\mu\text{m}$ . The recombinant endoglucanase (Endoglucanase, CelA) and anchoring region protein (Dockerin, docT) genes used were provided by the Department of Life Sciences, National Chung Hsing University (Taichung, Taiwan), and the Biodiversity Research Center, Academia Sinica (BRCAS, Taipei, Taiwan), respectively. The pET21b-CelA-docT-his plasmid was constructed by gene recombination technology in our laboratory (Figure S5). Moreover, *E. coli* DH5 $\alpha$  was used as host cells for gene transformation, and *E. coli* ER2566 and *E. coli* BL21 (DE3) were used as host cells for recombinant protein expression. The source of plasmid and *E. coli* strains are mentioned in Table S1.

#### 3.2. Gene Cloning and *E. coli* Culture

In this study, the endoglucanase (CelA) gene from the cellulosome of *Clostridium thermocellum* was expressed in *E. coli*. The competent cells to be used for transformation were prepared by using the heat shock method [50]. The procedure was performed under sterile conditions and at low temperatures. The transformation was achieved by adding plasmid DNA (pET21b-celA-docT-his) to 100  $\mu\text{L}$  of previously prepared competent cells. The contents were placed on ice for 30 min, and plasmid was allowed into the channel on the membrane by calcium ions. After this, the contents were placed in a dry bath at 42  $^{\circ}\text{C}$  for 2 min and immediately placed on ice for 3–5 min. The presence of the targeted gene in the plasmid DNA was detected by polymerase chain reaction (PCR) using gene-specific primers. Plasmid DNA from the recombinant cells was extracted using the QIAprep<sup>®</sup> Spin Miniprep Kit (QIAGEN, Hilden, Germany) and stored at  $-20^{\circ}\text{C}$ . The PCR-amplified product was subjected to agarose gel electrophoresis for the confirmation of gene fragment size.

#### 3.3. Gene Expression and Enzyme Extraction

After transformation, the bacterial cells were cultured on Luria–Bertani (LB) agar medium at 37  $^{\circ}\text{C}$ . A single colony was inoculated in 10 mL LB broth containing ampicillin (50  $\mu\text{g}/\text{mL}$ ) and incubated overnight at 37  $^{\circ}\text{C}$  and 200 rpm. For expression, 1% of the inoculum ( $\text{O.D}_{600} = 0.6\text{--}0.8$ ) to 100 mL was added to the LB broth medium and induced with IPTG (0.1–0.7 mM). The culture was incubated at 37  $^{\circ}\text{C}$  and 200 rpm for 6 h or 15  $^{\circ}\text{C}$  and 200 rpm for 24 h. Protein expression was confirmed with 10% SDS-PAGE.

The harvested broth was subjected to centrifugation at 4  $^{\circ}\text{C}/8500$  rpm for 10 min to separate the supernatant. The obtained pellet was dissolved in lysis buffer (pH 8.0, 20 mM, Tris-buffer) solution. The bacterial cells were broken by using an ultrasonic sterilizer at 45% amplitude with a pulse of 30 s on and 30 s off for 10 min. The suspension was then subjected to centrifugation at 4  $^{\circ}\text{C}/8500$  rpm for 20 min and the supernatant collected was considered crude CelA enzymes.

#### 3.4. Preparation of IMAMs and Enzyme Immobilization

IMAMs were prepared according to the method of Liu et al. [26]. A piece of the RC membrane was placed in a glass jar, followed by the addition of 20 mL of 1.4 M NaOH and 5 mL of EPI (activator). The solution was reacted at 24  $^{\circ}\text{C}/150$  rpm for 12 h. The membrane was washed three times with deionized water, and 20 mL of 1 M IDA (pH 11) was added thereafter. The reaction was carried out at 24  $^{\circ}\text{C}/100$  rpm for 12 h. The modified membrane was washed with deionized water 3 times. Before the chelation of metal ions to the IMAM membrane, the impact of various metal ions on the enzyme activity of recombinant free cellulase was determined. Different metal ions, viz.,  $\text{Zn}^{2+}$ ,  $\text{Al}^{3+}$ ,  $\text{Cu}^{2+}$ ,

$\text{Ni}^{2+}$ ,  $\text{Fe}^{3+}$ ,  $\text{Mn}^{2+}$ , and  $\text{Co}^{2+}$ , were used to study their effect on enzyme activity. The metal ion solution of concentrations of 1, 5, and 10 mM was used. The metal ion with a significant positive impact on enzyme activity was used to chelate the membrane by soaking the membrane in 20 mL of metal ion solutions at 25 °C for 2 h. The membrane was washed with deionized water 3 times to obtain IMAMs (Scheme 1). For enzyme immobilization, 20 mL (1.32 mg/mL) crude CelA with an activity of 1.25 U/mL was loaded onto one piece of IMAM and kept at 4 °C for 16 h. The scanning electron microscopy (SEM) images of the RC membrane before and after immobilization are shown in Figure S6.

### 3.5. Preparation of RC-EPI-DA-GA Membranes and Enzyme Immobilization

According to the method of Chen et al., a piece of the RC membrane was placed in a glass jar, 1.4 M NaOH (20 mL) and 5 mL EPI were added, and the reaction was carried out at 24 °C/150 rpm for 12 h [32]. After the reaction, the membrane was washed three times with deionized water, followed by the addition of 10 mL of 1 M DA (pH 11). The reaction was carried out at 24 °C for 12 h, and the membrane was washed with deionized water thrice. GA (10 mL of 0.1%, *v/v*) was used for activating the membrane. The membrane was incubated with GA at 25 °C for 2 h to obtain the RC-EPI-DA-GA membrane (Scheme 2). The impact of GA concentration and treatment time on enzyme activity was also determined. The enzyme was immobilized in the same manner as explained above.

### 3.6. Characterization of Thin Films by FTIR Analysis

The RC membranes before and after modification with EPI and IDA were subjected to FTIR characterization to directly measure the change in the functional group. FTIR analysis was carried out by using a Horiba FT-720 spectrometer (Horiba Ltd., Kyoto, Japan). The spectra (4000–400  $\text{cm}^{-1}$ ) were recorded with a resolution of 4  $\text{cm}^{-1}$ , and 64 scans were performed per sample.

### 3.7. Assays

The cellulolytic activity of the enzyme was determined by using carboxymethyl cellulose sodium salt (CMC) as a substrate. The amount of reducing sugars liberated was estimated by the 3,5-dinitrosalicylic acid (DNS) method [51]. Precisely, free enzymes (0.2 mL) and one immobilized membrane were separately mixed with 0.8 mL of 1% CMC solution and 10 mL of 1% CMC solution, respectively, and incubated in a water bath at 60 °C/100 rpm for 10 min. After incubation, the reaction mixture of free enzymes was mixed with 1 mL DNS, whereas for the immobilized membrane, 1 mL of the hydrolytic product was taken after incubation and mixed with 1 mL DNS. The reaction mixture was kept at 100 °C for 10 min. The mixture was cooled down after incubation by adding 8 mL of deionized water, and sugars were quantified by measuring absorbance at 540 nm. The amount of enzyme required to release one micromole of glucose per min was defined as one unit (IU) of enzyme activity. The protein estimation was done using the Bradford assay, with bovine serum albumin (BSA) as the standard [52].

### 3.8. Effect of pH and Temperature

The optimum pH of free and immobilized enzymes was estimated. The enzymes were incubated with CMC substrate prepared at varying pH values, i.e., pH 4–9, using Britton–Robinson buffer. The reaction was executed at 60 °C/100 rpm for 10 min, and then, enzyme activity was evaluated. The pH stability of the enzyme was also studied. Free and immobilized enzymes were pre-incubated at pH 4–9 for 2 h at 4 °C, followed by cellulase activity analysis. Similarly, optimum temperatures of free and immobilized enzymes were also assessed. The enzyme was incubated with CMC substrate (pH 6), and the reaction was executed at different temperatures (50–90 °C) and 100 rpm for 10 min, followed by enzyme activity analysis. For the thermo-stability analysis, free and immobilized enzymes were pre-incubated at temperatures of 50–90 °C for 1 h at pH 6, followed by cellulase activity analysis. Enzyme storage stability was also evaluated. Free and immobilized enzymes

were stored at 4 °C for 5, 10, and 15 days and an enzyme activity assay was performed. The ratio of the enzyme's activity to the maximum activity was used to determine the relative activity.

### 3.9. Kinetic Analysis

The Michaelis–Menten kinetic constant, i.e.,  $K_m$  and the maximal velocity rate  $V_{max}$ , was calculated for the free and immobilized enzymes using the Lineweaver Burk double reciprocal plot. The free and immobilized enzymes were allowed to react with varying CMC substrate concentrations. The activities obtained at different substrate concentrations were used to plot the Michaelis–Menten equation double reciprocal graph (Equation (1)). The linear relationship on this plot was used to calculate the maximum reaction rate ( $V_{max}$ ) and the Michaelis–Menten constant ( $K_m$ ).

$$\frac{1}{V_0} = \left( \frac{K_m}{V_{max}} \right) \left( \frac{1}{S_0} \right) + \frac{1}{V_{max}} \quad (1)$$

where  $S_0$  is the initial concentration of the substrate;  $V_0$  is the initial rate of the reaction;  $K_m$  is the Michaelis–Menten constant;  $V_{max}$  is the maximum rate of reaction.

### 3.10. Reusability Study for Immobilized CelA

To test the reusability of the immobilized CelA, a disc of the prepared CelA membrane was used. Prior to each reusability cycle, the membrane was taken out of the reaction mixture and washed twice with PBS buffer. The reaction conditions and the residual CelA activity on the membrane were determined according to the methods listed in Section 3.7. The relative activity was calculated as the ratio of the residual CelA activity after each use to that of the original activity.

### 3.11. IMAM Regeneration

The removal of immobilized enzymes and coupled metal ions is imperative for the regeneration of the IMAM membrane. Various stripping solutions, viz., EDTA, HCl, NaOH, and binding buffer, were used, and the feasibility of stripping using different agents was investigated. The membrane regeneration with imidazole was carried out by washing the membrane thrice with deionized water and soaking it in 10 mL of 250 mM imidazole solution for 30 min, followed by rinsing twice with phosphate buffer (PB, 25 mM, pH 8). For stripping with EDTA alone, the membrane was subjected to washing with deionized water three times and soaked in 10 mL, 100 mM EDTA for 1 h. It was then rinsed twice with phosphate buffer (25 mM, pH 8). Membrane regeneration using EDTA sequentially combined with HCl and/or NaOH was also executed. For EDTA + HCl, treatment with 100 mM EDTA was carried out, as explained above, followed by immersing the membrane in 10 mL 0.5 M HCl for 10 min and then washing twice with deionized water. Similarly, for EDTA + NaOH, after soaking the membrane in 100 mM EDTA and washing, it was dipped in 10 mL 0.5 M NaOH for 10 min. For regeneration using combined EDTA + HCl + NaOH, the membrane was sequentially treated with each chemical, as explained above, and washed twice after every treatment. Finally, to complete the regeneration process for each treatment, the membrane was soaked in 10 mL binding buffer (300 mM NaCl, 25 mM PB buffer, pH 8) for 20 min [49]. The regeneration efficiency was evaluated by coupling metal ions and immobilizing the enzyme again to the membrane, as described in Section 3.4, after regenerating the membrane with different solutions, alone or in combination.

## 4. Conclusions

The current study is the first to report the immobilization of recombinant endoglucanase (CelA) on RC membranes modified using two different approaches, i.e., RC-EPI-IDA- $Co^{2+}$  (IMAM) and RC-EPI-DA-GA. FTIR analysis revealed the successful modification of the RC membrane using EPI-IDA and DA-GA. The immobilization improved the temperature (50–90 °C) stability of the enzyme compared to free enzymes, whereas the pH (4–9)

stability of free and immobilized enzymes was similar as both displayed approximately 80% relative activity. Enzyme immobilization aided in enzyme reusability, which is a crucial factor in maintaining the economic sustainability of the process. The immobilized enzyme was effectively used for five cycles, with 63% and 53% of relative activity for RC-EPI-IDA-Co<sup>2+</sup>-CelA and RC-EPI-DA-GA-CelA, respectively. Moreover, the coupling of Co<sup>2+</sup> ions on the IMAM increased the enzyme activity and preliminary purification due to the RC-EPI-IDA-Co<sup>2+</sup>-CelA immobilization, leading to a 3.19-fold purification, followed by RC-EPI-DA-GA-CelA (1.54-fold purification). In comparison with free enzymes, the enzyme immobilized on the membrane had better kinetic characteristics ( $K_m$  and  $V_{max}$ ). An effective five-times regeneration of RC-EPI-IDA-Co<sup>2+</sup> was achieved with almost 100% activity. Although both approaches of immobilization improved enzyme characteristics and efficacy, RC-EPI-IDA-Co<sup>2+</sup> showed a better performance than the RC-EPI-DA-GA-modified membrane for CelA immobilized with respect to purification and reusability. Therefore, IMAM immobilization emerges as a potential approach for increasing enzyme efficacy and reusability.

**Supplementary Materials:** The following supporting information can be downloaded at: <https://www.mdpi.com/article/10.3390/catal12111356/s1>, Figure S1: DNA electropherogram of pET21b-CelA-his plasmid in *E. coli* BL21 (a) and *E. coli* ER2566 (b), confirmed by gene cleavage. Lane M: 1 Kb marker; Lane 1–3: CelA digested with Nde I and Xho I, Figure S2: Effects of different metal ions on the activity of CelA endoglucanase enzyme, Figure S3: Effect of GA treatment time on CelA endoglucanase activity, Figure S4: SDS-PAGE electrophoresis of the His-tag-purified CelA. Lane M: marker (kDa); Lane 2: crude CelA; Lane 3: purified CelA, Figure S5: pET21b-CelA-docT gene construction; Figure S6: SEM micrographs of IMAM RC membrane (a) before (b) after immobilization; Table S1: *Escherichia coli* strains and plasmids used in the study.

**Author Contributions:** Conceptualization, Y.-C.L.; methodology, Z.-H.W.; validation, P.N.; formal analysis, Z.-H.W.; investigation, Z.-H.W.; writing—original draft preparation, P.N., C.-H.K. and Y.-C.L.; writing—review and editing, P.N., C.-H.K. and Y.-C.L.; supervision, Y.-C.L. All authors have read and agreed to the published version of the manuscript.

**Funding:** This study was supported by the Ministry of Science and Technology of Taiwan (grant no. MOST 108-2221-E-005-041-MY2).

**Data Availability Statement:** Data are contained within the article.

**Conflicts of Interest:** The authors declare no conflict of interest.

## References

1. Sharma, V.; Tsai, M.-L.; Chen, C.-W.; Sun, P.-P.; Patel, A.K.; Singhania, R.R.; Nargotra, P.; Dong, C.-D. Deep eutectic solvents as promising pretreatment agents for sustainable lignocellulosic biorefineries: A review. *Bioresour. Technol.* **2022**, *360*, 127631. [[CrossRef](#)] [[PubMed](#)]
2. Patel, S.K.; Kalia, V.C.; Joo, J.B.; Kang, Y.C.; Lee, J.K. Biotransformation of methane into methanol by methanotrophs immobilized on coconut coir. *Bioresour. Technol.* **2020**, *297*, 122433. [[CrossRef](#)] [[PubMed](#)]
3. Nargotra, P.; Sharma, V.; Bajaj, B.K. Consolidated bioprocessing of surfactant-assisted ionic liquid-pretreated *Parthenium hysterophorus* L. biomass for bioethanol production. *Bioresour. Technol.* **2019**, *289*, 121611. [[CrossRef](#)] [[PubMed](#)]
4. Amjith, L.; Bavanish, B. A review on biomass and wind as renewable energy for sustainable environment. *Chemosphere* **2022**, *293*, 133579. [[CrossRef](#)] [[PubMed](#)]
5. Sharma, S.; Nargotra, P.; Sharma, V.; Bangotra, R.; Kaur, M.; Kapoor, N.; Paul, S.; Bajaj, B.K. Nanobiocatalysts for efficacious bioconversion of ionic liquid pretreated sugarcane tops biomass to biofuel. *Bioresour. Technol.* **2021**, *333*, 125191. [[CrossRef](#)] [[PubMed](#)]
6. Kumari, D.; Singh, R. Pretreatment of lignocellulosic wastes for biofuel production: A critical review. *Renew. Sustain. Energy Rev.* **2018**, *90*, 877–891. [[CrossRef](#)]
7. Vasić, K.; Knez, Ž.; Leitgeb, M. Bioethanol production by enzymatic hydrolysis from different lignocellulosic sources. *Molecules* **2021**, *26*, 753. [[CrossRef](#)]
8. Kuo, C.-H.; Lee, C.-K. Enhanced enzymatic hydrolysis of sugarcane bagasse by N-methylmorpholine-N-oxide pretreatment. *Bioresour. Technol.* **2009**, *100*, 866–871. [[CrossRef](#)]
9. Patel, S.K.; Singh, M.; Kumar, P.; Purohit, H.J.; Kalia, V.C. Exploitation of defined bacterial cultures for production of hydrogen and polyhydroxybutyrate from pea-shells. *Biomass Bioenergy* **2012**, *36*, 218–225. [[CrossRef](#)]

10. Vadala, B.S.; Deshpande, S.; Apte-Deshpande, A. Soluble expression of recombinant active cellulase in *E. coli* using *B. subtilis* (natto strain) cellulase gene. *J. Genet. Eng. Biotechnol.* **2021**, *19*, 1–7. [[CrossRef](#)]
11. Hosseini, S.H.; Hosseini, S.A.; Zohreh, N.; Yaghoubi, M.; Pourjavadi, A. Covalent immobilization of cellulase using magnetic poly (ionic liquid) support: Improvement of the enzyme activity and stability. *J. Agric. Food Chem.* **2018**, *66*, 789–798. [[CrossRef](#)]
12. Gennari, A.; Fühler, A.J.; Volpato, G.; de Souza, C.F.V. Magnetic cellulose: Versatile support for enzyme immobilization—A review. *Carbohydr. Polym.* **2020**, *246*, 116646. [[CrossRef](#)] [[PubMed](#)]
13. Kumar, V.; Patel, S.K.; Gupta, R.K.; Otari, S.V.; Gao, H.; Lee, J.K.; Zhang, L. Enhanced saccharification and fermentation of rice straw by reducing the concentration of phenolic compounds using an immobilized enzyme cocktail. *Biotechnol. J.* **2019**, *14*, 1800468. [[CrossRef](#)]
14. Jia, J.; Zhang, W.; Yang, Z.; Yang, X.; Wang, N.; Yu, X. Novel magnetic cross-linked cellulase aggregates with a potential application in lignocellulosic biomass bioconversion. *Molecules* **2017**, *22*, 269. [[CrossRef](#)] [[PubMed](#)]
15. Kuo, C.-H.; Liu, Y.-C.; Chang, C.-M.J.; Chen, J.-H.; Chang, C.; Shieh, C.-J. Optimum conditions for lipase immobilization on chitosan-coated Fe<sub>3</sub>O<sub>4</sub> nanoparticles. *Carbohydr. Polym.* **2012**, *87*, 2538–2545. [[CrossRef](#)]
16. Patel, S.K.; Anwar, M.Z.; Kumar, A.; Otari, S.V.; Pagolu, R.T.; Kim, S.Y.; Kim, I.W.; Lee, J.K. Fe<sub>2</sub>O<sub>3</sub> yolk-shell particle-based laccase biosensor for efficient detection of 2,6-dimethoxyphenol. *Biochem. Eng. J.* **2018**, *132*, 1–8. [[CrossRef](#)]
17. Kuo, C.-H.; Chen, G.-J.; Twu, Y.-K.; Liu, Y.-C.; Shieh, C.-J. Optimum lipase immobilized on diamine-grafted PVDF membrane and its characterization. *Ind. Eng. Chem. Res.* **2012**, *51*, 5141–5147. [[CrossRef](#)]
18. Singh, R.S.; Chauhan, K.; Kaur, N.; Kumar, N. Inulinase immobilization onto glutaraldehyde activated duolite XAD for the production of fructose from inulin. *Biocatal. Agric. Biotechnol.* **2020**, *27*, 101699. [[CrossRef](#)]
19. Patel, S.K.; Choi, S.H.; Kang, Y.C.; Lee, J.K. Large-scale aerosol-assisted synthesis of biofriendly Fe<sub>2</sub>O<sub>3</sub> yolk-shell particles: A promising support for enzyme immobilization. *Nanoscale* **2016**, *8*, 6728–6738. [[CrossRef](#)]
20. Patel, S.K.; Choi, H.; Lee, J.K. Multimetal-based inorganic–protein hybrid system for enzyme immobilization. *ACS Sustain. Chem. Eng.* **2019**, *7*, 13633–13638. [[CrossRef](#)]
21. Nargotra, P.; Sharma, V.; Sharma, S.; Bangotra, R.; Bajaj, B.K. Purification of an ionic liquid stable cellulase from *Aspergillus aculeatus* PN14 with potential for biomass refining. *Environ. Sustain.* **2022**, *5*, 313–323. [[CrossRef](#)]
22. Wong, H.-L.; Hu, N.-J.; Juang, T.-Y.; Liu, Y.-C. Co-immobilization of xylanase and scaffolding protein onto an immobilized metal ion affinity membrane. *Catalysts* **2020**, *10*, 1408. [[CrossRef](#)]
23. Cheung, R.C.F.; Wong, J.H.; Ng, T.B. Immobilized metal ion affinity chromatography: A review on its applications. *Appl. Microbiol. Biotechnol.* **2012**, *96*, 1411–1420. [[CrossRef](#)] [[PubMed](#)]
24. Xi, C.R.; Di Fazio, A.; Nadvi, N.A.; Patel, K.; Xiang, M.S.W.; Zhang, H.E.; Deshpande, C.; Low, J.K.; Wang, X.T.; Chen, Y. A novel purification procedure for active recombinant human DPP4 and the inability of DPP4 to bind SARS-CoV-2. *Molecules* **2020**, *25*, 5392. [[CrossRef](#)] [[PubMed](#)]
25. Wu, C.-Y.; Suen, S.-Y.; Chen, S.-C.; Tzeng, J.-H. Analysis of protein adsorption on regenerated cellulose-based immobilized copper ion affinity membranes. *J. Chromatogr. A* **2003**, *996*, 53–70. [[CrossRef](#)]
26. Liu, Y.-C.; ChangChien, C.-C.; Suen, S.-Y. Purification of penicillin G acylase using immobilized metal affinity membranes. *J. Chromatogr. B* **2003**, *794*, 67–76. [[CrossRef](#)]
27. Kim, D.; Ku, S. Bacillus cellulase molecular cloning, expression, and surface display on the outer membrane of *Escherichia coli*. *Molecules* **2018**, *23*, 503. [[CrossRef](#)]
28. Zhou, Y.; Lu, Z.; Wang, X.; Selvaraj, J.N.; Zhang, G. Genetic engineering modification and fermentation optimization for extracellular production of recombinant proteins using *Escherichia coli*. *Appl. Microbiol. Biotechnol.* **2018**, *102*, 1545–1556. [[CrossRef](#)]
29. Huleani, S.; Roberts, M.R.; Beales, L.; Papaioannou, E.H. *Escherichia coli* as an antibody expression host for the production of diagnostic proteins: Significance and expression. *Crit. Rev. Biotechnol.* **2022**, *42*, 756–773. [[CrossRef](#)]
30. Mühlmann, M.; Forsten, E.; Noack, S.; Büchs, J. Optimizing recombinant protein expression via automated induction profiling in microtiter plates at different temperatures. *Microb. Cell Factories* **2017**, *16*, 1–12. [[CrossRef](#)]
31. Lin, T.-N.; Lin, S.-C. Metal chelate-epoxy bifunctional membranes for selective adsorption and covalent immobilization of a His-tagged protein. *J. Biosci. Bioeng.* **2022**, *133*, 258–264. [[CrossRef](#)] [[PubMed](#)]
32. Chen, G.-J.; Kuo, C.-H.; Chen, C.-I.; Yu, C.-C.; Shieh, C.-J.; Liu, Y.-C. Effect of membranes with various hydrophobic/hydrophilic properties on lipase immobilized activity and stability. *J. Biosci. Bioeng.* **2012**, *113*, 166–172. [[CrossRef](#)] [[PubMed](#)]
33. Modenez, I.A.; Sastre, D.E.; Moraes, F.C.; Marques Netto, C.G. Influence of glutaraldehyde cross-linking modes on the recyclability of immobilized lipase B from *Candida antarctica* for transesterification of soy bean oil. *Molecules* **2018**, *23*, 2230. [[CrossRef](#)] [[PubMed](#)]
34. Hua, C.; Li, W.; Han, W.; Wang, Q.; Bi, P.; Han, C.; Zhu, L. Characterization of a novel thermostable GH7 endoglucanase from *Chaetomium thermophilum* capable of xylan hydrolysis. *Int. J. Biol. Macromol.* **2018**, *117*, 342–349. [[CrossRef](#)] [[PubMed](#)]
35. Chaga, G.S. Twenty-five years of immobilized metal ion affinity chromatography: Past, present and future. *J. Biochem. Biophys. Methods* **2001**, *49*, 313–334. [[CrossRef](#)]
36. Li, T.; Gong, X.; Yang, G.; Li, Q.; Huang, J.; Zhou, N.; Jia, X. Cross-linked enzyme aggregates (CLEAs) of cellulase with improved catalytic activity, adaptability and reusability. *Bioprocess Biosyst Eng.* **2022**, *45*, 865–875. [[CrossRef](#)]
37. Zeng, R.; Jin, B.K.; Yang, Z.H.; Guan, R.; Quan, C. Preparation of a modified crosslinked chitosan/polyvinyl alcohol blended affinity membrane for purification of his-tagged protein. *J. Appl. Polym. Sci.* **2019**, *136*, 47347. [[CrossRef](#)]

38. Ahmad, R.; Khare, S.K. Immobilization of *Aspergillus niger* cellulase on multiwall carbon nanotubes for cellulose hydrolysis. *Bioresour. Technol.* **2018**, *252*, 72–75. [[CrossRef](#)]
39. Kaur, P.; Taggar, M.S.; Kalia, A. Characterization of magnetic nanoparticle-immobilized cellulases for enzymatic saccharification of rice straw. *Biomass Convers. Biorefin.* **2021**, *11*, 955–969. [[CrossRef](#)]
40. Saleem, M.; Rashid, M.; Jabbar, A.; Perveen, R.; Khalid, A.; Rajoka, M. Kinetic and thermodynamic properties of an immobilized endoglucanase from *Arachniotus citrinus*. *Process Biochem.* **2005**, *40*, 849–855. [[CrossRef](#)]
41. Guo, R.; Zheng, X.; Wang, Y.; Yang, Y.; Ma, Y.; Zou, D.; Liu, Y. Optimization of cellulase immobilization with sodium alginate-polyethylene for enhancement of enzymatic hydrolysis of microcrystalline cellulose using response surface methodology. *Appl. Biochem. Biotechnol.* **2021**, *193*, 2043–2060. [[CrossRef](#)] [[PubMed](#)]
42. Abbaszadeh, M.; Hejazi, P. Metal affinity immobilization of cellulase on Fe<sub>3</sub>O<sub>4</sub> nanoparticles with copper as ligand for biocatalytic applications. *Food Chem.* **2019**, *290*, 47–55. [[CrossRef](#)]
43. Saha, K.; Verma, P.; Sikder, J.; Chakraborty, S.; Curcio, S. Synthesis of chitosan-cellulase nanohybrid and immobilization on alginate beads for hydrolysis of ionic liquid pretreated sugarcane bagasse. *Renew. Energy* **2019**, *133*, 66–76. [[CrossRef](#)]
44. Wang, Y.; Feng, C.; Guo, R.; Ma, Y.; Yuan, Y.; Liu, Y. Cellulase immobilized by sodium alginate-polyethylene glycol-chitosan for hydrolysis enhancement of microcrystalline cellulose. *Process Biochem.* **2021**, *107*, 38–47. [[CrossRef](#)]
45. Singh, S.; Gupta, P.; Bajaj, B.K. Characterization of a robust serine protease from *Bacillus subtilis* K-1. *J. Basic Microbiol.* **2018**, *58*, 88–98. [[CrossRef](#)]
46. Chien, H.-I.; Tsai, Y.-H.; Wang, H.-M.D.; Dong, C.-D.; Huang, C.-Y.; Kuo, C.-H. Extrusion puffing pretreated cereals for rapid production of high-maltose syrup. *Food Chem. X* **2022**, *15*, 100445. [[CrossRef](#)]
47. Tüzmen, N.; Kalburcu, T.; Denizli, A. Immobilization of catalase via adsorption onto metal-chelated affinity cryogels. *Process Biochem.* **2012**, *47*, 26–33. [[CrossRef](#)]
48. Zhu, H.; Zhang, Y.; Yang, T.; Zheng, D.; Liu, X.; Zhang, J.; Zheng, M. Preparation of immobilized Alcalase based on metal affinity for efficient production of bioactive peptides. *LWT* **2022**, *162*, 113505. [[CrossRef](#)]
49. Chen, C.-I.; Ko, Y.-M.; Lien, W.-L.; Lin, Y.-H.; Li, I.-T.; Chen, C.-H.; Shieh, C.-J.; Liu, Y.-C. Development of the reversible PGA immobilization by using the immobilized metal ion affinity membrane. *J. Membr. Sci.* **2012**, *401*, 33–39. [[CrossRef](#)]
50. Morrison, D. Transformation and preservation of competent bacterial cells by freezing. In *Methods in Enzymology*; Elsevier: Amsterdam, The Netherlands, 1979; Volume 68, pp. 326–331.
51. Miller, G.L. Use of dinitrosalicylic acid reagent for determination of reducing sugar. *Anal. Chem.* **1959**, *31*, 426–428. [[CrossRef](#)]
52. Bradford, M.M. A rapid and sensitive method for the quantitation of microgram quantities of protein utilizing the principle of protein-dye binding. *Anal. Biochem.* **1976**, *72*, 248–254. [[CrossRef](#)]